energies

MDPI

Article

Performance and Economic Assessment of a Grid-Connected Photovoltaic Power Plant with a Storage System: A Comparison between the North and the South of Italy

Ferdinando Chiacchio [1,*], Fabio Famoso [2], Diego D'Urso [1] and Luca Cedola [3]

[1] Department of Electrical, Electronical and Computer Engineering, University of Catania, Viale Andrea Doria 6, 95025 Catania, Italy; ddurso@diim.unict.it
[2] Department of Civil Engineering and Architecture, University of Catania, Viale Andrea Doria 6, 95025 Catania, Italy; ffamoso@unict.it
[3] Department of Mechanical and Aerospace Engineering, University of Rome, Via Eudossiana 18, 00184 Roma, Italy; luca.cedola@uniroma1.it
* Correspondence: chiacchio@dmi.unict.it

Received: 29 May 2019; Accepted: 16 June 2019; Published: 19 June 2019

Abstract: Grid-connected low voltage photovoltaic power plants cover most of the power capacity installed in Italy. They offer an important contribution to the power demand of the utilities connected but, due to the nature of the solar resource, the night-time consumption can be satisfied only withdrawing the energy by the national grid, at the price of the energy distributor. Thanks to the improvement of storage technologies, the installation of a system of battery looks like a promising solution by giving the possibility to increase auto-consumption dramatically. In this paper, a model-based approach to analyze and discuss the performance and the economic feasibility of grid-connected domestic photovoltaic power plants with a storage system is presented. Using as input to the model the historical series (2008–2017) of the main ambient variables, the proposed model, based on Stochastic Hybrid Fault Tree Automaton, allowed us to simulate and compare two alternative technical solutions characterized by different environmental conditions, in the north and in the south of Italy. The performances of these systems were compared and an economic analysis, addressing the convenience of the storage systems was carried out, considering the characteristic useful-life time, 20 years, of a photovoltaic power plant. To this end the Net Present Value and the payback time were evaluated, considering the main characteristics of the Italian market scenario.

Keywords: renewable energy; Stochastic Hybrid Automaton; Monte Carlo simulation; cash-flow analysis; net present value; discounted payback time

1. Introduction

In the last decades, the photovoltaic industry has grown world-wide. Nowadays, small and decentralized photovoltaic (PV) power plants play a key role in the sustainable development of distributed generation and will become one of the main pillars of the smart-grid and smart-city revolution [1]. While the feasibility analysis of large photovoltaic power plants can be very complex, low voltage (LV) systems that represent most domestic applications are characterized by a great simplicity of design, installation, and operation. For these reasons, their diffusion has strongly increased in these last years, supported also by government incentive policies and technical regulations. These latter have required the interconnection of the PV power plant with the national electrical grid [2] with a twofold objectives: To guarantee the energy supply of households when the PV system does

not produce, and to allow the injection of the unused energy into the electrical grid that can be seen as a virtual battery of infinitive capacity. This type of architecture takes the name of *grid-connected* power plants.

The economic advantage of the PV investments has been investigated in several works [3–6] under different viewpoints. In [3] the determinants of investment risk in the PV industry was analyzed, and alternative business plans were evaluated in order to quantify how Net Present Value (NPV) varies according to different parameters. Edalati et al. [4] studied the technical and economic feasibility of a 10 MW_p grid-connected PV power plant located in Iran, having performed a comparison of profit expectations in different cities. The feed-in tariff (FIT) profit of a 5 kW_p photovoltaic power plant, considering an annual update of the tariff with a 30% reduction during the second decade of the investment, has been studied by Bakhshi and Sadeh [5]. In [6], Cucchiella et al. proposed an economic analysis that considers residential households with different consumptions and levels of insolation in order to evaluate several well-known indicators such as NPV, Discounted Payback Time (DPBT), and Levelized Cost of Electricity (LCOE), and pointed out that the success of the PV sector is linked to subsidies. According to these studies, it appears evident that the diffusion of grid-connected PV systems has provided great benefits not only in terms of social and environmental impact but has represented also a valuable economic investment for the community [7].

The PV market scenario analyzed in the previous works is characterized by grid-connected PV power plants able to produce during the daylight hours but unable to store the unused energy. But, most of the energy household consumption occurs during the night-time and is satisfied by withdrawing energy from the electrical grid. For these reasons, in many countries, the mechanism of the feed-in-tariff (FIT) has been adopted and tuned [8] in order to favor these type of investments and guarantee to the power plant owners an economic benefit that can compensate the exchange of energy (required and injected to and from the grid) and subsidize the investment of the PV installation. In these last few years, favored by a reduction of the production costs and by an increase in performance, the storage systems have become particularly attractive also within the PV market. In [9], an in-depth overview about the market and technology development of home storage systems in Germany during the years 2013–2018 is presented, showing that the rapid growth of installations has concerned the domestic power plant segment (<6 kWp). Akinyele et al. [10] perform a comparison among several storage system technologies for stand-alone PV systems, demonstrating that storage systems can favor independence from the electrical grid. On the other hand, it must be pointed out that grid-connected configurations have the great advantage of drastically reducing the interruption of energy supply (that can occur in stand-alone PV systems) and, with the installation of a storage system, incrementing the auto-consumption, limiting the energy withdrawal from the grid. Therefore, for this latter configuration, a performance and an economic evaluation of the whole system (i.e., power plant, storage system, and electrical grid connection) can aid the correct sizing of the PV system (peak power, inverter, storage system capacity) and to understand the economic benefits, with respect to household consumption and the environmental characteristics of the power plant location. In [11], Abdin and Noussan presented a thorough economic analysis to evaluate, in the Italian market, the differences between a PV power plant working under the net-metering regime and the same configuration equipped with different (in size) type of storage systems. In this study, they revealed that the NPV of a PV system with a storage system, after ten years, will always be negative. In fact, at the state of the art, the costs of storage technologies are still considerable, and the return on investment can really depend on the specific geographical market, as shown in [11,12]. In an earlier work [13], a domestic grid-connected photovoltaic power plant located in the south of Italy was analyzed so as to assess the performance for only one year of operations. Due to the short period of investigation, the main contribution of [13] is not the obtained results, but the application of a Dynamic Reliability [14,15] modelling—to gather in a single model the physical and the stochastic processes characterizing the functioning of a system. In [16], the benefits of the Tesla Powerwall battery were investigated for PV power plants located in Germany, demonstrating that three key-factors—(i) the price gap between the electricity

price and the remuneration rate, (ii) the battery system's investment cost, and (iii) the usable battery capacity—strongly influenced the feasibility of the investment. Therefore, it appears clear that ad-hoc studies that consider the market of the country, the geographical sites, and specific consumptions profiles are of great interest for researchers and practitioners.

In this paper, the analysis of a domestic grid-connected PV power plant equipped with a storage system has been performed considering two different geographical sites, located in the north and in the south of Italy. The first objective of this study is to evaluate how different environmental conditions, in the north and in the south of Italy, can affect not only the energy production and the self-consumption regimes, but also the aging of the components with particular emphasis on the storage system.

The model of the case of study has been designed using a Stochastic Hybrid Fault Tree Automaton (SHyFTA) [17–19]. One of the main contributions of this paper has been the utilization of this modelling technique that allows for the account of the physical process of energy conversion and for the stochastic process of failure and repair of the system components (like the aging of the battery, inverter, and PV panels as proposed in [20–24]). Moreover, the SHyFTA model can be coded in order to take as input real variables and, in this study, it was possible to use the historical series of the global irradiation and of the ambient temperature of the last ten years (2008–2017) for both the locations selected.

The second objective of this study is to analyze and compare the economic feasibility of the PV power plants with and without a battery, working within the net-metering regime. Therefore, a thorough economic analysis that considers the Italian market scenario and the technical regulations of the grid-connected PV power plant is presented. The simulations have been extended to twenty years in order to compare the NPV and the DPBT.

The rest of this paper is organized as follows. Section 2 describes the basic concepts of the PV conversion and the main working principles of a PV storage system. In Section 3, the case study of the domestic grid-connected PV power plant is presented. Section 4 illustrates the SHyFTA model adopted to simulate the PV system, the main results of the simulation analysis, and, finally, the economic assessment. Section 5 contains a discussion and the final conclusions.

2. Model of Photovoltaic Conversion and Battery Storage

The performance assessment of a PV system can be carried out by the means of a mathematical model. Literature provides [3–12] several contributions that show how the complexity of a model depends on the objectives of the performance assessment, on the modeling hypotheses, and on the available modeling inputs. For instance, the most trivial model must be able to evaluate the expected yearly energy production by the knowledge of the mean solar irradiation. More complex models can include other factors like the deterioration of the system components, the maintenance activities, and the related economic aspects.

As a first approximation, the electrical power P generated with a simple configuration (same tilt and orientation for all modules) [21] can be defined as follows:

$$P = \eta I_o \sin(\alpha) S \tag{1}$$

where I_0 is the orthogonal solar irradiance to the direction of solar radiation (W/m^2); α is the angle of the module/string with respect to the incident solar radiation; S is the area of the module (m^2); and η is the system efficiency that is always less than 1.

The total efficiency of a PV power plant can be expressed as:

$$\eta = \prod_{i=1}^{n} \eta_i \tag{2}$$

where n is the number of loss effects considered at each ith stage of the power plant (inverter, cables, breakers, etc.).

The main dynamic efficiency degradation process depends on meteorological factors such as wind speed, cloud transients in PV units, incident irradiance and ambient temperature. Ref. [16,21] propose a yearly deterioration model that is able to account for the most common meteorological factor, including the ambient temperature. Using Equation (3), it is possible to compute the efficiency of the module, η_m, by considering the variation of the temperature [21]:

$$\begin{cases} \eta_m = \eta_{std}\left\{1 - \rho(T_c - T_{c,std})\right\} \\ \frac{T_c - T_a}{G} = \text{constant} \end{cases} \quad (3)$$

where η_{std} and $T_{c,std}$ are respectively the efficiency and the module temperature at standard conditions (STC), ρ is the power coefficient (percentage variation of power for 1 °C), Tc and Ta are the module and ambient temperatures and G is the global irradiance on the module.

To account for the degradation rate, Dr, corresponding with the percentage of efficiency lost every year [22], it is possible to use a linear equation model:

$$\eta_n = \eta_{first}(1 - nD_r) \quad (4)$$

where η_{first} is the nominal efficiency at the first year, while η_n is the efficiency calculated at the n^{th} year.

As already said, other components are involved in the process of energy conversion performed by a PV system, like protections, cables, breakers, disconnectors, and inverters. All these components play an important role in the energy production because if one of them interrupts the circuit path to the grid, the PV generator stops producing. For a grid-connected PV plant, as the one proposed in the case study, another circumstance causing the production to stop is a disconnection from the electrical grid inside the grid stage. Therefore, these events must be considered in order to achieve a realistic model of a PV generation system.

The energy produced and measured can be calculated by integrating the power produced in the time interval [t2, t1]:

$$E(t) = \int_{t1}^{t2} P(t)dt \quad (5)$$

In recent PV applications, it has become popular to integrate storage equipment—systems able to store the unused energy produced by the PV plant and not instantaneously consumed by the electrical equipment (household utilities).

An energy storage system can be modelled according to its degradation behavior, during its entire lifetime. The lifetime of the batteries (especially Li-ion technologies) [23] varies depending on their thermal environment and how they are charged and discharged. While technical datasheets usually declare a typical usable lifetime of 10 years or more (i.e., approximately 3650 cycles), they do not point at the degradation process. Usually Li-ion battery lifetime depends on many factors, such as battery operating and storage temperatures, depth of discharge (DoD) and state of charge (SoC), as shown in Figure 1. Many authors have investigated these factors, both theoretically and with semi-empirical models. Christensen et al. [23] developed a cycling-driven generation model to predict fracture in active electrode material of Li-ion cells. Deshpande et al. [24] coupled electrochemistry and chemical degradation to model life performance of Li-ion cells. Other authors [25–29] have faced the dynamic aging by conducting test data to real-world battery scenarios according to different levels of complexity and parameters. In the work proposed here, the dynamic aging was adapted from a previous study [29], on the degradation behavior of Li-Ion batteries. The correspondent SoC and DoD was calculated for each cycle (see Figure 1). As suggested in [29], lifetime models that are able to estimate the capacity fade of Li-ion battery cell for cycling in various conditions, are given by Equation (6) for a cycling temperature of 25 °C (the Li-ion batteries used in grid support services are operated most of the time at

25 °C by means of air-conditioning systems). Therefore, in the model of the battery aging, Equations (6) and (7) have been used:

$$C_{fc} = 0.021e^{-0.01943*SoC} * cd^{0.7162} * nc^{0.5} \quad (6)$$

$$P_{dc} = 1.1725 * 10^{-6} * cd^{0.7891} * nc \quad (7)$$

where C_{fc} is the capacity fade at the given cycle, nc represents the number of cycles and cd represents the depth of the cycle. In Equation (7), P_{dc} represents te power capability decrease during the considered cycle.

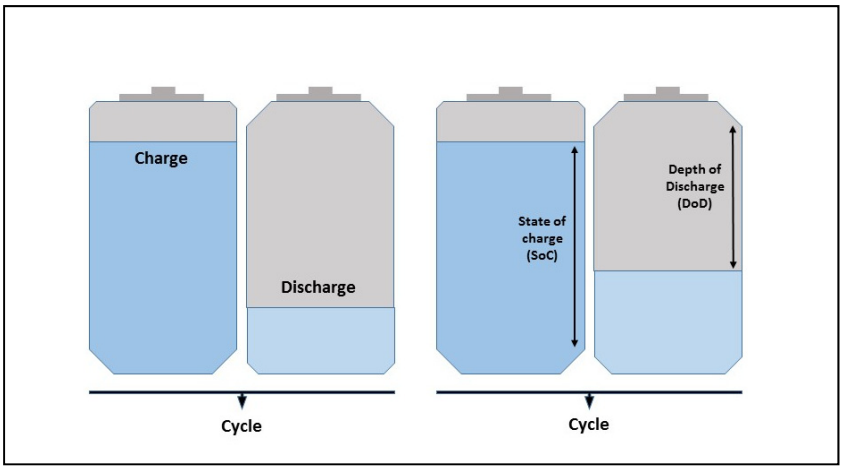

Figure 1. The battery cycle working principle, state of charge (SoC) and depth of discharge (DoD).

3. Results

In this paper, a case study of a grid-connected domestic photovoltaic plant equipped with a battery is analyzed. The main PV plant components are the PV panels, the AC/DC inverter, and the storage system. Figure 2 shows the working scheme of the system.

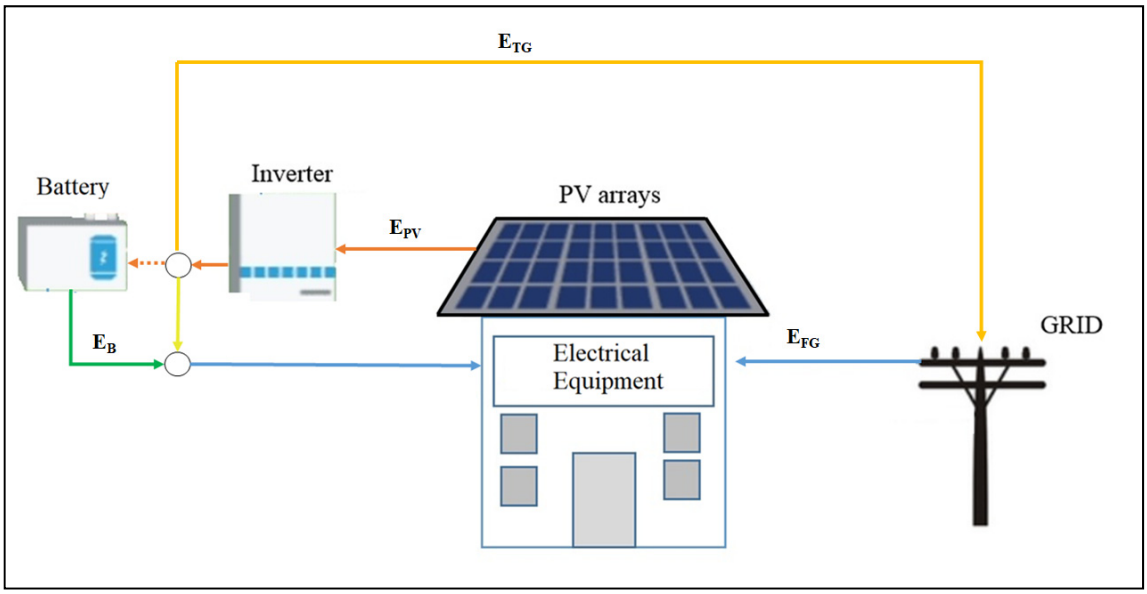

Figure 2. The PV plant working scheme.

In the proposed scheme, the domestic energy demand of the "Electrical Equipment" is satisfied, hierarchically, according to the following operation conditions:

- From the PV energy production (E_{PV}) whenever the plant is working (and producing);
- from the battery storage system (E_B) if the demand exceeds the instantaneous PV production;
- from the electrical grid (E_{FG}) in all the other cases.

At the same time, the main working principles of the battery are summarized according the following logic:

- Charging: When an excess of power produced by the PV plant is available and the battery is not fully charged. In this case, the instantaneous charging power can be computed as the difference between the PV production and the power required by the electrical equipment.
- Discharging: As soon as the electrical equipment needs power and the instantaneous PV plant production is not sufficient to fulfill this demand. This condition is likely to happen during the night, since the PV plant does not produce electricity then.

Moreover, if the battery is full and the instantaneous PV plant production exceeds the power demand of the electrical equipment, this excess power is injected to the grid, (E_{TG}), according the net-metering regulations [11].

From the description of the working scheme so far provided, it is possible to understand that in a grid-connected power plant, the electrical grid plays a fundamental role. In fact, it behaves as a virtual spare battery of infinitive capacity that, on the one hand, collects the instantaneous power produced by the PV plant that is not instantaneously consumed by the household equipment and, on the other hand, provides the energy required by the household utilities when the PV plant and the battery are not able to fulfill these requests. In many countries, the net-metering regulations [11] discipline the management and economic aspects of the mechanisms of energy-exchange between a PV power plant and the electrical grid.

In Italy, an important technical feature of the grid-connected PV is an automatic safety mechanism of disconnection (generally installed within the inverter), in case of fault of the electrical grid. This mechanism stops the functioning of the PV system (PV plant and battery) and represents the worst-case scenario for the energy supply of the household. In fact, in these cases, the energy demand cannot be fulfilled by any of the three main supplier (PV plant, battery and grid).

In the following, the main characteristics of the PV plant object of the case of study are shown. A common size (P_{peak} = 3 kW) of a domestic PV plant was considered. In this configuration, it constituted of 10 panels (each one of 300 W) in series. The main technical information of a single panel is shown in Table 1, whereas Table 2 resumes the characteristics of the AC/DC.

Table 1. Main characteristics of photovoltaic (PV) panels.

PM_{peak}	300 (W) (Sy-Poly)
Module area	1.9 (m^2)
Panel efficiency (η)	15%
I_{sc}	8.8 (A)
I_{mpp}	8.4 (A)
V_{mp}	37 (V)
V_{oc}	50 (V)
NOCT	45 ± 2 (°C)

Table 2. Main characteristics of the inverter.

P_{acmax}	2.8 (kW)
Efficiency (η)	97%
Max DC Voltage	550 (V)
Max DC Current	13.5 (A)
MPP(T) range	210–550 (V)

The main characteristics of the battery are presented in Table 3. In the proposed case of study, the battery was characterized by a capacity of 6.4 kWh (80% DOD).

Table 3. Main characteristics of the storage system.

E_s	6.4 (kWh) (Lithium-Ion)
Global capacity	134 (Ah)
Battery voltage	50 (V)
Charge cut-off voltage	58.8 (V)
Discharge cut-off voltage	35 (V)
Maximum charging current	64 (A)
Maximum discharging current	64 (A)
Minimum charging temperature	0 (°C)
Minimum discharging temperature	−20 (°C)

The PV power plant analysis was performed considering two different geographical sites of Italy in order to investigate two different environmental conditions. This allowed us to simulate two working conditions for the whole PV system (PV plant, inverter, and battery) which affected not only the energy production, but also the self-consumption regimes, the system aging, and, ultimately, the economic aspects.

Table 4 summarizes the main details of the proposed investigated sites. The assessment process was conducted in accordance with a provided input data of ambient temperature (T_a) and irradiation (I) of 10 years (2008–2017) for both sites with a time step of 1 h, for a total of 87,672 samplers. Data for Location 2 were provided from [30], while data for Location 1 were provided from [31]. Data was pretreated in order to handle missing values (less than 1% for both sites). A Python script was implemented in order to replace missing values with a moving average calculation (by considering similar time and seasonal intervals subsets).

Table 4. The geographical cases of study.

	Location 1	Location 2
Position	45°28′ N 9°12′ E	37°31′ N 15°04′ E
IG_y	~1500 kWh/m^2	~2000 kWh/m^2
P_{peak}	3 kW$_p$	3 kW$_p$
Azimuth Angle (β)	180°	180°
N° modules	10	10
E_S	6.4 kWh	6.4 kWh
Tilt	30°	30°

Figure 3 shows the trends of the household energy demand, characterizing a generic day of each season of the year. The mean yearly consumption sums up to about 3750 kWh.

In order to obtain the seasonal average consumption profiles, the authors have considered the main equipment of a household, living in a house making full use of electricity with air-conditioners used during winter and summer. A third-party software for calculating these consumption profiles was used. The software required the number of the main electrical appliances and the following equipment were considered: Air-conditioner (n.2), television (n.2), washing machine (n.1), dryer (n.1), and computer (n.2). Moreover, general consumptions due to lighting was automatically calculated.

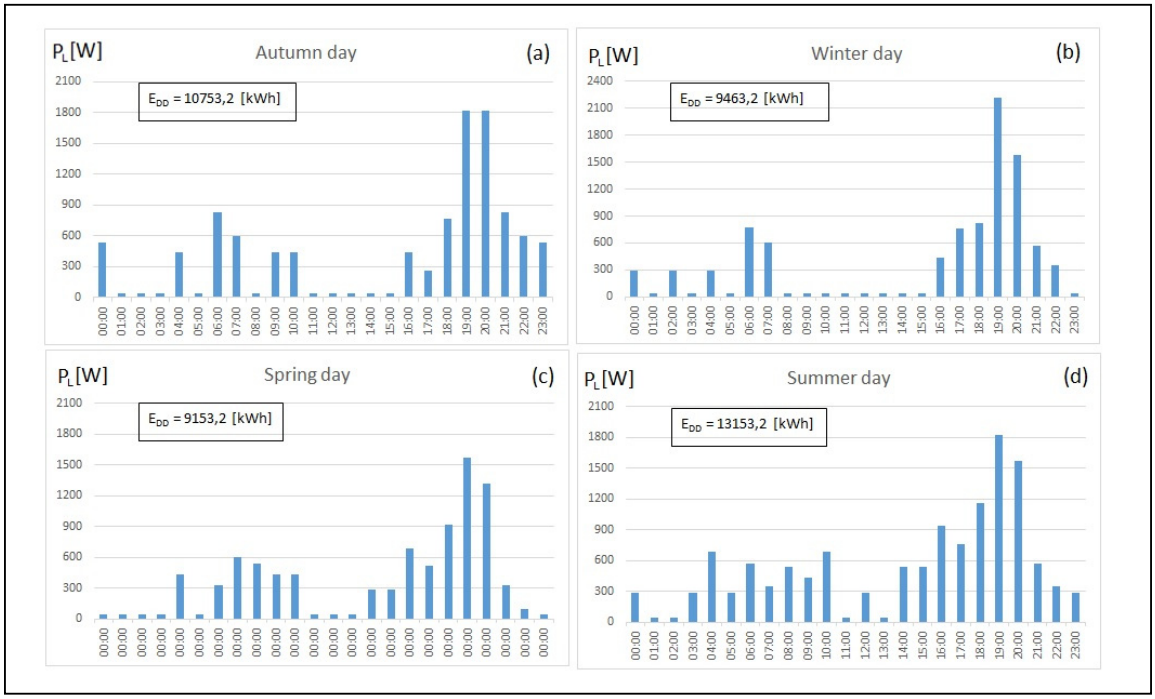

Figure 3. The energy demand proposed for each season: (**a**) Autumn, (**b**) Winter, (**c**) Spring, (**d**) Summer.

4. Simulation Model and Results

In a previous work [19], a Stochastic Hybrid Fault Tree Automaton (SHyFTA) was used to model a large-scale photovoltaic power plant and assess the service availability and the main dependability means. The same formalism was adopted in [13] to present a preliminary study for the performance evaluation of a domestic photovoltaic power plant with a storage system. The aim of these researches was to demonstrate the effectiveness of this modelling technique. But, in terms of quantifiable results, the main limitation of these analyses was the short time-horizon (five and one year, respectively), although it is known that photovoltaic power plants have an average life of twenty years. As aforementioned, in this research paper it was possible to obtain the historical time-series of the solar irradiation and environmental temperature of the last ten years (2008–2017) of two locations in Italy, therefore a more realistic and thorough analysis could be performed.

In the next sections, the SHyFTA modelling formalism will be used in order to illustrate the model of the photovoltaic system in the simulation. The main results will be presented so as to point out the main differences in terms of performance between the two geographic locations. Moreover, an economic assessment comparing the investment linked to the installation of a PV system, with and without battery, will be presented.

4.1. Stochastic Hybrid Fault Tree Automaton

Stochastic Hybrid Fault Tree Automaton (SHyFTA) is a modelling formalism that belongs to the umbrella of Dynamic Reliability [14,15], an engineering science that aims to study a system by the use of an holistic model that is able to consider the physics of the system process and its inter-relationships with the system dependability, (i.e., the probability of a system performing its task under some specifications like operative conditions, time of mission, restoration, maintenance resources, and so forth [32]).

SHyFTA is a formalism based on the separation of concerns [17] which allows us to break the modelling of a system process into two inter-dependent sub-models, the deterministic and the stochastic, that are coupled by the mean of shared variables. This simplifies the conception of complex models. Figure 4 shows the coupling between the deterministic and the stochastic processes.

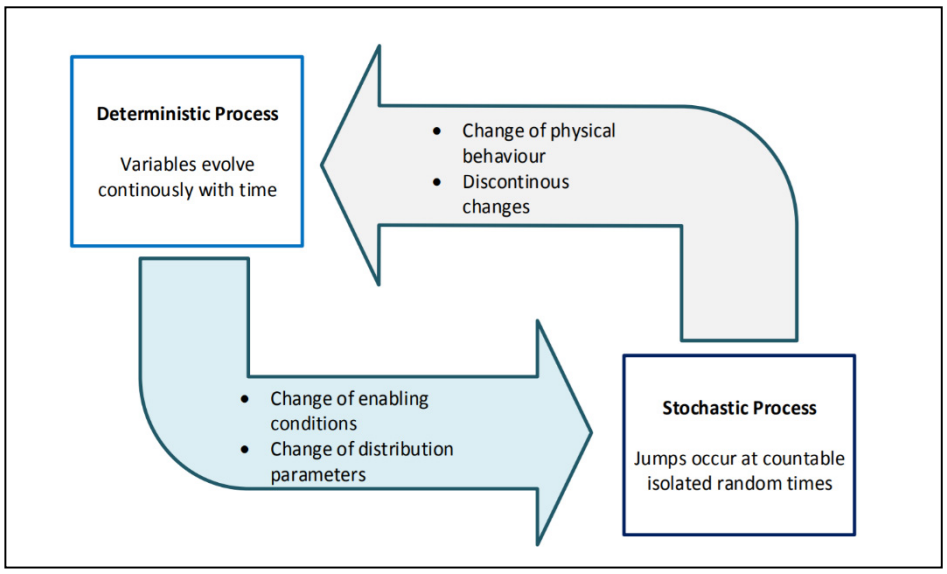

Figure 4. Coupling of the deterministic and stochastic process by mean of shared variables.

In the SHyFTA formalism, the deterministic model can be described with the mathematical equations of the system process, whereas the stochastic model takes the form of a Dynamic Fault Tree. The graphical representation of a fault tree is a logic diagram constituted by a Top Event (TE), Basic Events (BEs), and Gates. Following a TOP-DOWN approach, the construction of a DFT is realized by identifying the sequence of events that brings into occurrence the TE. The TE is the undesired scenario of the fault tree. On the other hand, BEs are the leaves of the fault tree and represent the elementary events of a process, generally linked with the failure of the system components. Gates are used to logically interconnect the BEs and/or other intermediary events, originated by the triggering of other gates.

The shared variables allow the coupling of these two inter-dependent sub-models so that a variation of the deterministic dynamic can arouse a change on the parameters of the stochastic sub-model and vice-versa. Typical interrelationships between the deterministic to the stochastic model are the variations of the working conditions that can alter the failure behavior of the system. On the other hand, the most common shared variables of the stochastic model affecting the deterministic dynamics are the components status: If a component gets deteriorated (or even broken), its contribution within the deterministic process is nullified.

To implement a SHyFTA model, the modeler must identify the components that participate to the physical process and realize the DFT schema that, on the other hand, describes the system failure logic of the system. For the energy supply system of the household shown in Figures 2, 5 and 6 present the deterministic (or physical) and the stochastic diagram (the DFT) of the SHyFTA model. As it is shown, the Basic Events of the DFT represent the active components of the physical model.

In this paper, the implementation and resolution of the SHyFTA model was achieved exploiting a software toolbox library (SHyFTOO) running under the Matlab® framework.

4.2. SHyFTA Model of the Household Energy Supply

The SHyFTA model hereby presented depicts the process of energy supply for a generic household equipped with a grid-connectected photovoltaic power plant and a storage system. The deterministic schema of the process, in Figure 5, allows the identification of the main sub-systems: The photovoltaic power plant (PV Generator), the storage system (BAT), and the equipment of the grid connection coupling (GCC) that allow the coupling with the electrical grid.

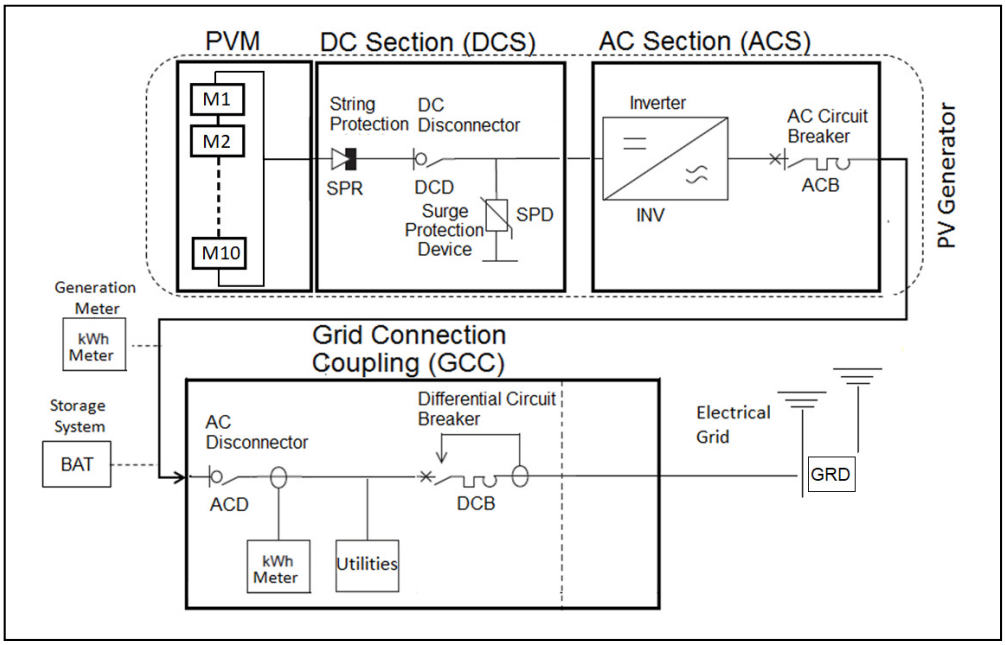

Figure 5. Schema of the deterministic process of the PV system, including the battery.

In detail, they can be decomposed into the following functional blocks:

1. **PV Module (PVM)**, made up by ten photovoltaic modules (M1–M10);
2. **Direct Current Section (DCS)**, made up of string protection diodes (SPR), a DC disconnector (DCD), and a surge protection device (SPD);
3. **Alternating Current Section (ACS)**, made up of an inverter (INV) and an AC circuit breaker (ACB);
4. **Grid Connector Coupling (GCC)**, made up of an AC disconnector (ACD), a differential circuit breaker (DCB), and a generic sub-system representing the electrical grid (GRD).
5. **Battery (BAT)** that is connected in parallel in the AC section.

As already said in Section 3, for management reasons, a grid-connected power plant must be connected to the national electrical grid. If the electrical grid fails, the power plant must be disconnected, stopping the production and the energy supply of the household. Moreover, in these cases, the battery is also forbidden to supply energy to the household until the grid has recovered. This scenario corresponds to the top event of the Dynamic Fault Tree shown in Figure 6. This model is constituted by the Top Event AND gate (TE) that takes as input the output of the OR gate GCC (OR (ACD, DCB, GRD)) and the OR gate PV Fault (OR (ACS, DCS)). The former models any type of disconnection of the electrical grid, whereas the latter the unavailability of the photovoltaic power plant that occurs if the electrical circuit of the PV Generator gets open (any failure of the ACS or DCS components). The AND Gate PVM models the failure of the photovoltaic strings; although the modules are connected in series, the by-pass diodes guarantee the electrical isolation of those modules that are not working properly.

As far as it concerns the battery, it must be pointed that its unavailability does not cause a stop of the household energy supply because the grid can fulfill the energy request. On the other hand, likewise the PV power plant operativity, any disconnection from the electrical grid causes the unavailability of the battery. These behaviors can be modelled with the DFT using a FDEP Gate, taking as primary input the output of the GCC and secondary inputs the BAT and the OR Gate of the PV Fault.

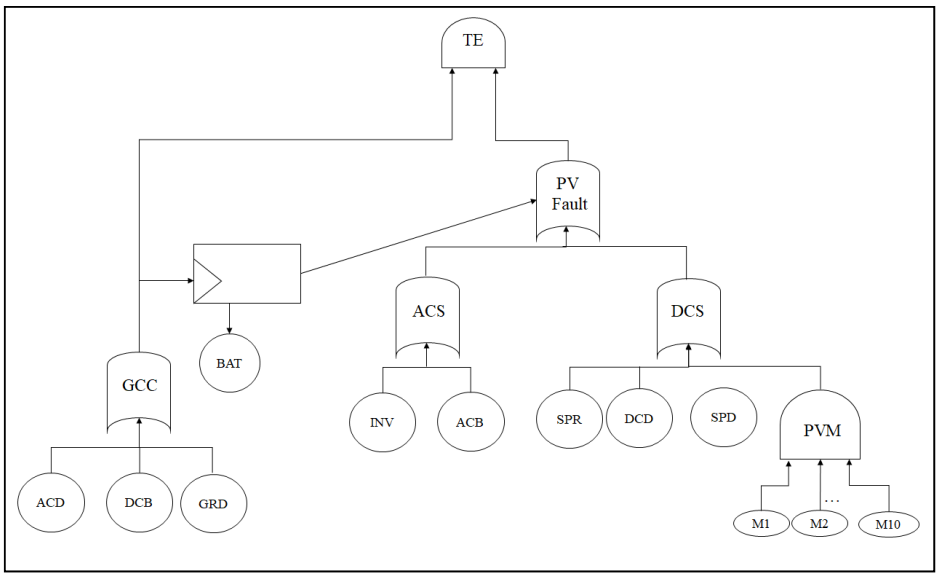

Figure 6. Dynamic Fault Tree (DFT) of the energy supply of a domestic household equipped with a PV system.

As generally assumed in the literature, failure and restoration of the system components follow the exponential probability density function that model a random failure/repair. Table 5 shows the parameters adopted. Failures are measured in occurrence per year whereas repairs in occurrence per hour. As for repair rates, it was assumed that electrical components such as breakers and disconnectors can be restored as-good-as-new within 12 h, string box and surge protections within 48 h after fault. A failure of the grid is restored within four hours, whereas more critical components like the inverter, the battery and the modules, according to the agreements with the manufacturers, are repaired within three or four weeks, so as to consider the whole process of inspection, ordering, delivery, and replacement.

Table 5. Failure/repair rates and of the photovoltaic power plant.

	Component	λ: Failure Rate (year^{-1})	μ: Repair Rate (h^{-1})
Mi	PV Module	1/15	1.4×10^{-3}
SPR	String Protection	1/10	1/48
DCD	DC Disconnector	1/3	1/12
SPD	Surge Protection	1/10	1/48
INV	Inverter	1/10	2.1×10^{-3}
ACB	AC Circuit Breaker	1/10	1/12
ACD	AC Disconnector	1/3	1/12
DCB	Diff. Circuit Breaker	1/3	1/48
GRD	Grid	5	1/4
BAT	Storage System	1/15	2.1×10^{-3}

The SHyFTA model was coded with the SHyFTOO library under the Matlab® and Simulink framework. The Matlab script used to create the DFT is shown in Table 6 (parameters have to be defined in number of occurrences per hour).

The physical process can be developed in Simulink, exploiting the built-in blocks available in the Simulink libraries. Thanks to the SHyFTOO library, the coupling between the physical and the stochastic model was easily realized, exploiting the properties of the SHyFTOO components that were used as shared variables. For instance, Figure 7 shows the PVM section: Ten modules (M1–M10) contributed to the conversion of the solar irradiation. The generic block "Mi_Status" (i = 1, i = 2, . . . , i = 10) took as input the status of the module from the stochastic process. If the status of the

generic module was not good, its contribution was nullified in the "Interpreted MATLAB Fcn" that implemented the physical equations shown in Equations (1)–(4). It was possible to identify the other inputs of these equations: (1) The simulation clock, (2) the historical series of the solar irradiation, and (3) the ambient temperature. In this way, the equations can compute at any instant of the simulation the power produced by the solar string. Clearly, the physical process is not limited to the previous block but, since the Simulink model is not the main object of this paper, the rest of the blocks are not illustrated.

Table 6. DFT model syntax with the SHyFTOO library.

Define the Fault Tree Structure
1: Tm = 87,672; %10 years of operations in (h)
2: %% Define BEs %%
3: ACB = BasicEvent('ACB','exp','exp',[3.8e-5],[1/12]); %break 1 in 3 year; repair 1 in 12 h
4: ACD = BasicEvent('ACD','exp','exp',[3.8e-5],[1/12]); %break 1 in 3 year; repair 1 in 12 h
5: DCD = BasicEvent('DCD','exp','exp',[3.8e-5],[1/12]); %break 1 in 3 year; repair 1 in 12 h
6: SPR = BasicEvent('SPR','exp','exp',[1.14e-5],[1/48]);%break 1 in 10 year; repair 1 in 48 h
7: SPD = BasicEvent('SPD','exp','exp',[1.14e-5],[1/48]);%break 1 in 10 year; repair 1 in 48 h
8: DCB = BasicEvent('DCB','exp','exp',[1.14e-5],[1/48]);%break 1 in 10 year; repair 1 in 48 h
9: INV = BasicEvent('INV','exp','exp',[1.14e-5],[2.1e-3]); %break 1 in 10 year; repair 1 in 20 days
10: BAT = BasicEvent('BAT','exp','exp',[7.61e-6],[2.1e-3]); %break 1 in 15 year; repair 1 in 20 days
11: [M1, M2, . . . , M10] = deal(BasicEvent('M1','exp','exp',[7.61e-6],[1.4e-3])); 1; %break 1 in 15 years; repair 1 in 30 days
12: GRD = BasicEvent('GRD','exp','exp',[5/8760],[1/4]); %break 5 in 1 year; repair 1 in 4 h
13: % %% Define Gates %%
14: PVM = Gate ('PVM', 'AND', false, [M1,M2,M3,M4,M5,M6,M7,M8,M9,M10]);
15: ACS = Gate ('ACS', 'OR', false, [INV, ACB]);
16: DCS = Gate ('DCS', 'OR', false, [PVM, DCD,SPD,SPR]);
17: PVFault = Gate('PVFault', 'OR', false, [ACS,DCS]);
18: GCC = Gate ('GCC', 'OR', false, [ACD, DCB, GRD]);
19: FDEP1 = Gate('FDEP1','FDEP', false, [GCC, BAT,PVFault]);
20: TE = Gate ('TE', 'AND', false, [GCC, PVFault]);

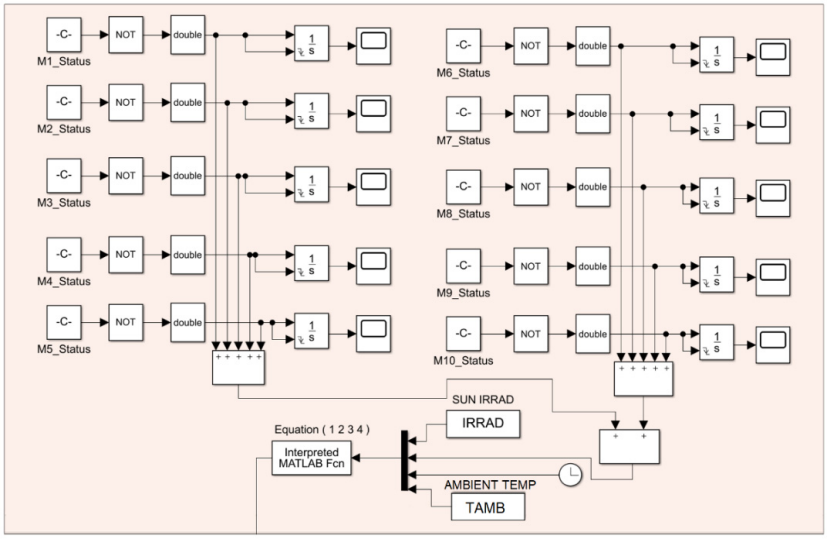

Figure 7. Simulink implementation of the PVM section.

4.3. Simulation Results

In order to evaluate the impact of the battery on the auto-consumption and on the energy withdrawn from the electrical grid, four main scenarios were simulated and compared, as summarized in Table 7. The simulations were built upon the cases of study described in Section 3, characterized by

two different geographical locations with the same photovoltaic system (peak nominal power and battery). As already mentioned, the historical time series collected data from 2008 to 2017, therefore the results presented in this section are related to ten years of simulation (corresponding to 87,672 h of operation).

Table 7. Simulation scenarios.

Id	Battery	Site
1	Y	Location 1
2	N	Location 1
3	Y	Location 2
4	N	Location 2

The measures of interest for the two locations were (1) the energy produced by the photovoltaic power plant E_{PV}, (2) the energy transferred to the grid E_{TG}, (3) the energy required and withdrawn by the grid E_{FG}, and (4) the loss of energy production E_L, due to the energy supply system unavailability (grid and PV system). It is worth reminding that E_{PV} and E_L are independent from the battery.

Figure 8 compares the energy produced for both the two locations. It is noticeable that in the Location 2, the expected production E_{PV} is higher than in the Location 1; if compared to the energy required by the household utilities, it can be seen that the design peak power (3 kW) would be enough to cover the consumption only in the Location 2 (and not in the Location 1). Figure 9 shows the production loss E_L due to the unavailability of the energy supply system. These value amounts to about the 2% of the energy produced that can be explained by the very high availability (0.9876) of the energy supply system, that can be computed with the stochastic failure process (e.g., the DFT) of the SHyFTA model.

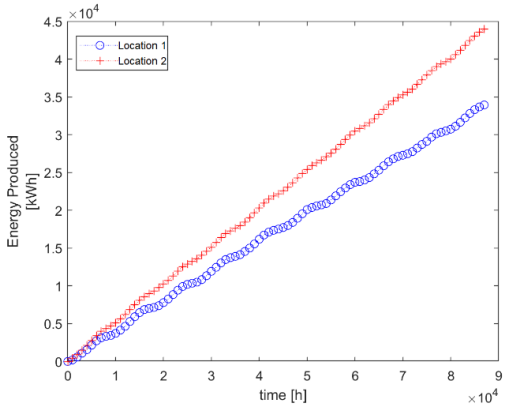

Figure 8. Energy produced.

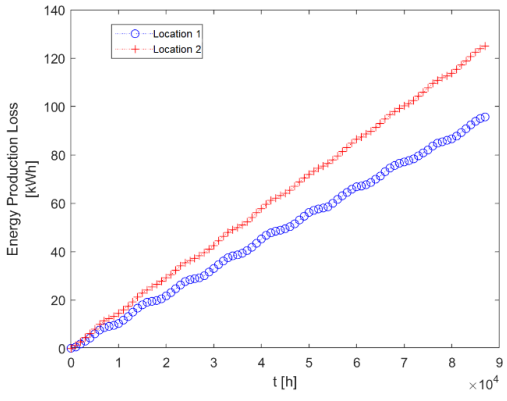

Figure 9. Energy production loss.

The energy withdrawn from the grid E_{FG}, needed to satisfy the utilities consumptions, is shown in Figures 10 and 11, respectively, for a PV system with and without the battery. In this case, as expected, the energy withdrawn from the grid is higher in Location 1, although this difference is less evident for the plant configuration without battery (Figure 11). This last behavior can be explained considering that household consumption are mostly concentrated during the second half of the day (late afternoon to night) when the power plants do not produce in both the locations.

The same trends are shown in Figures 12 and 13 but grouped with respect to the location. In both the cases, it is possible to notice that the battery increased dramatically the auto-consumption, reducing the energy request from the grid by about 50% in both the locations.

The energy transferred to the grid E_{TG} because it was not instantaneously consumed by the household utilities is shown in Figures 14 and 15.

Beside the fact that, as expected, the power plant of Location 2 injects to the grid more energy than the power plant of Location 1, an interesting fact is observed in Figures 16 and 17. In fact, they show the same trends with respect to the same location but highlighting, in the right axis, the percentage of the E_{PV} instantaneously transferred to the grid, which gives origin to the E_{TG}.

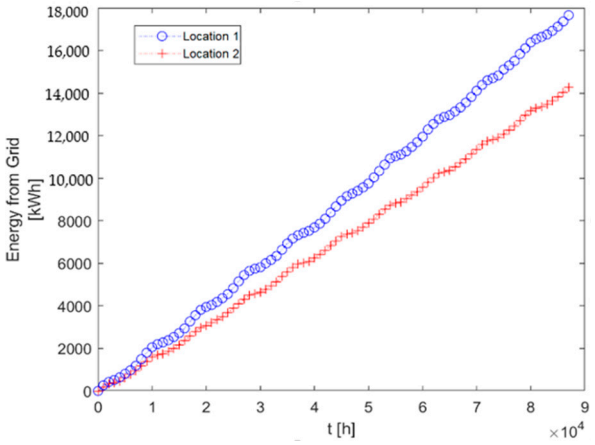

Figure 10. Energy from the grid (PV with battery).

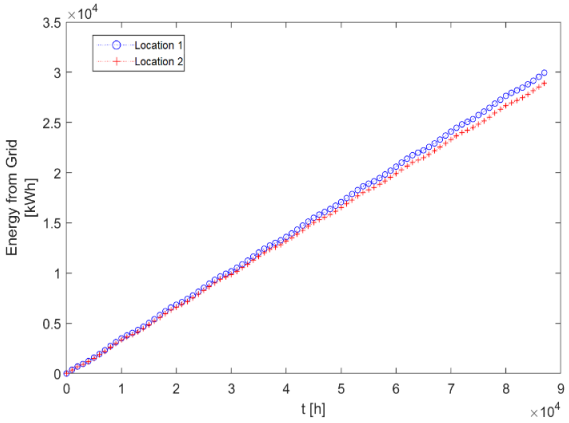

Figure 11. Energy from the grid (PV without battery).

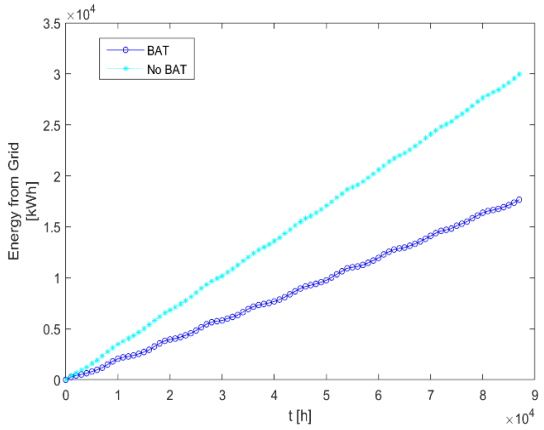

Figure 12. Energy request from the grid (Location 1).

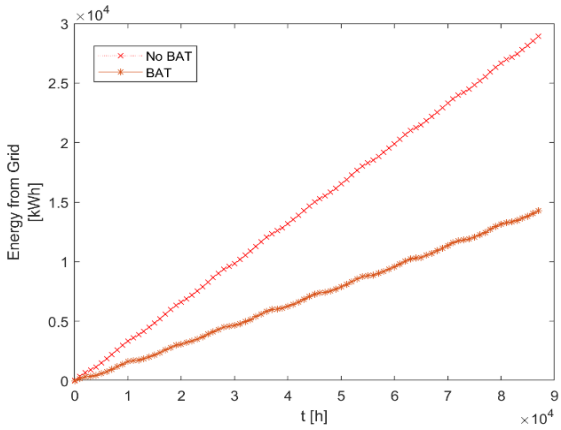

Figure 13. Energy request from the grid (Location 2).

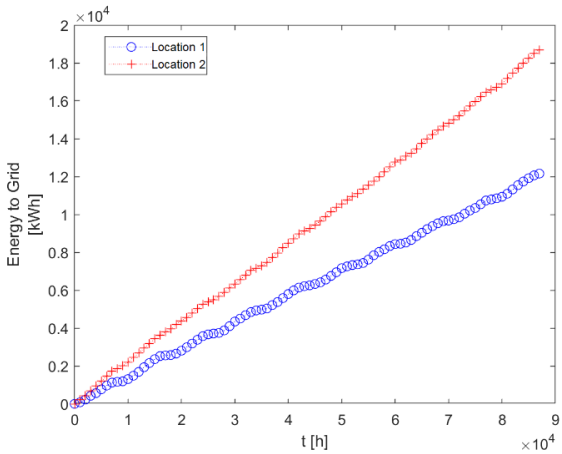

Figure 14. Energy to the grid (PV with battery).

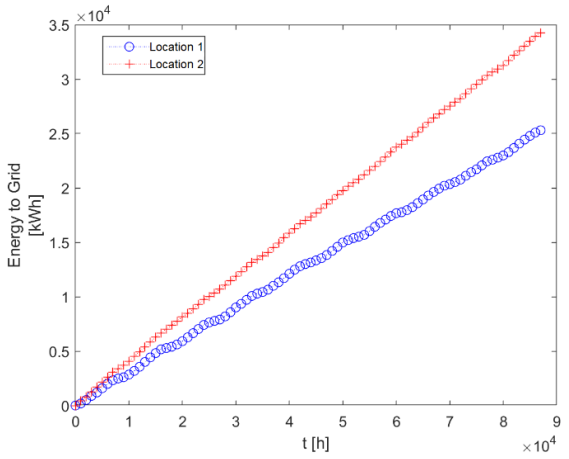

Figure 15. Energy to the grid (PV no battery).

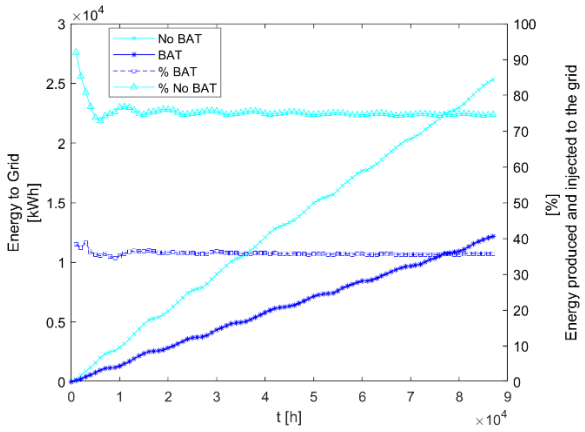

Figure 16. Energy to the grid (Location 1).

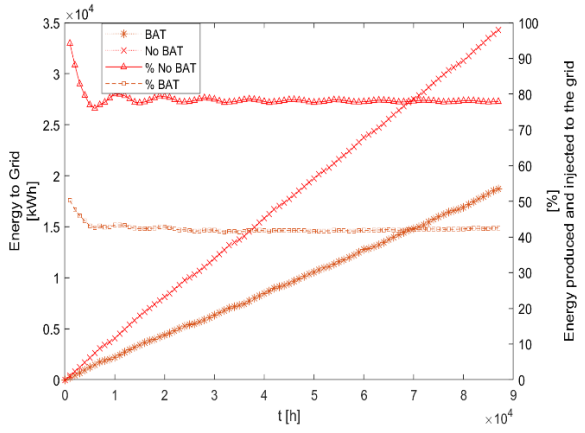

Figure 17. Energy to the grid (Location 2).

Although the percentage of unused E_{PV} is drastically reduced, the energy injected to the grid, E_{TG}, is still very high (approximately around the 40% of the energy produced by the power plant in both the locations). In order to reduce the ETG, the most appropriate way would be the increasing of the storage system capacity. But this option has a cost and, as it will be shown in the next section, the economic viewpoint cannot be disregarded.

4.4. Economic Assessment

As expected, the results of the simulations presented in Section 4.3 have shown that the installation of the battery increases the auto-consumption and, accordingly, decreases the withdrawal of energy from the electrical grid. Now, the main point to evaluate is whether the installation of the battery is convenient not only in terms of self-consumption but, above all, from an economic point of view.

In a similar work [11], an economic analysis targeting the Italian market showed that the profitability of an investment of a PV power plant equipped with a storage system is questionable, resulting with a payback time higher than 75 years. These results are very discouraging; therefore, in our study, it was decided to extend the simulation in order to consider a "Project Lifetime" of twenty years and to compare the "Net Present Value" [6] of two design configurations of a photovoltaic power plant with and without a battery. Clearly, some further assumption was needed and the main characteristics of the Italian PV market were considered for estimating the installation costs of a PV system and the costs of the electrical bill. Besides all, it must be observed that in the last decades the Italian market has been one of the most responsive to the photovoltaic offer, thanks to several government-sponsored subsidies that have included, among them, incentives and tax deductions. Therefore, the evaluations hereby summarized can provide valuable and interesting prompts for understanding the market and, in particular, the potential of storage system technology in domestic applications.

Table 8 shows the costs related to the installation and the contract management of a grid-connected photovoltaic power plant subjected to the net-metering regime (known also as SSP) [11]. They reflect the costs of an ordinary mono-phase low-voltage contract.

Table 8. Costs of PV installation, subscription to the net-metering service and dismission.

Item	Cost Type	Recurrence	Value
PV plant	Investment	Una tantum	2500 €/kWp
(Lithium) battery	Investment	Una tantum	500 €/kWh
Connection with the grid	Investment	Una tantum	120 €
Fee subscription for SSP	Investment	Una tantum	56 €
Annual fee for SSP	Service	Annual	30 €/year

The investment costs are related to the installation of the PV power plant and are sustained one time at the beginning of the investment (at the beginning of the first year). The annual costs refer to the net-metering service subscription (also known as SSP). In Table 9, the main components of the electrical bill are summarized.

Table 9. Costs of the electrical bill identifying fixed and variable components.

Item	Cost Type	Recurrence	Value
Fixed Price of Energy *	Fixed	+Annual	48 €/y
Price for the Metering Unit *	Fixed	+Annual	20 €/y
Power Costs *	Fixed	+Annual	21 €/kW
Energy Cost *	Variable	Monthly	0.06634 €/kWh
Additional Energy Cost L (≤1800 kWh/year) *	Variable	Monthly	0.035026 €/kWh
Additional Energy Cost H (>1800 kWh/year) *	Variable	Monthly	0.078394 €/kWh
Excise Duty	Taxes	Monthly	0.0227 €/kWh
VAT	Taxes	Monthly	10% of the bill

* it is assumed that every year these costs increase of the 1%; + the Annual costs are spread in the electrical bill every month.

The "Fixed Price of Energy", "Price for the Metering Unit", and "Power Costs" are annual costs sustained for the energy supply (contract with the energy provider). They are included and spread in the periodic electrical bill (every month) that also includes the costs linked with the amount of energy (kWh) EFG withdrawn from the grid. This latter is a variable whom unitary cost value depends on the

"Energy Cost" plus an "Additional Energy Cost" that is applied as follows: As long the yearly EFG is lower than 1800 kWh, the unitary cost is incremented with the value of the "Additional Energy Cost L" per kWh. Afterwards, the unitary cost per kWh is further increased using the "Additional Energy Cost H" (e.g., the auto-consumption limits these costs). The "Excise Duty" and the "VAT" are additional taxes payed on top of the bill.

Table 10 provides further data needed for the economic assessment.

Table 10. Further economic assumptions.

Item	Value
Energy Trade Price *	0.06 €/kWh
Unitary Fixed Exchange Value (UFEV or CUSF)	0.075 €/kWh
Discount Rate (r)	2.5%
Project Lifetime (investment horizon)	20 years

* it is assumed an annual increase of the 1%.

The "Unitary Fixed Exchange Value" is a mean of the variable components paid in the electrical bill, while the "Energy Trade Price" corresponds with the sales value of the energy produced by the power plant and transferred to the grid (e.g., energy not instantaneously used). These values are used to evaluate the net-metering contribution (or SSP). Since, they are slightly volatile (depends on the energy market), they have been fixed considering the current market scenario. Finally, the "Discount Rate" (r = rb + rr + r′) is defined according to the following economic scenario assumptions:

- r_b = 0.5%, is the borrowing/lending rate of interest. In our case, it was assumed an economic scenario of liquidity (lending rate).
- r_r = 1% is an interest rate featuring the industrial plant risk assessment. In our case, it was assumed a low value because PV technology is mature.
- r' = 1% is the liquidity risk premium.

Since the "Project Lifetime" has been set to twenty years, the analysis presented in the previous sections was extended accordingly; therefore, the Monte Carlo simulation was modified so as to shuffle, for the missing ten years, the historical time-series available.

The discounted cash flow method for the evaluation of the NPV is based on the cash-flows generated by an investment. Therefore, the NPV (20 year, 2.5%) was computed for the four scenarios of Table 11 with the formula:

$$\mathrm{NPV} = -\mathrm{C}_0 + \sum_{\mathrm{i}=1}^{\mathrm{PL}} \mathrm{CFD}_\mathrm{i} = -\mathrm{C}_0 + \sum_{\mathrm{i}=1}^{\mathrm{PL}} \frac{\mathrm{CF}_\mathrm{i}}{(1+\mathrm{r})^\mathrm{i}} = -\mathrm{C}_0 + \sum_{\mathrm{i}=1}^{\mathrm{PL}} \frac{(\mathrm{R}_\mathrm{i} + \mathrm{AC}_\mathrm{i})}{(1+\mathrm{r})^\mathrm{i}} \tag{8}$$

where C_0 are the costs sustained for the installation and the start-up of the photovoltaic system (at the beginning of the investment) and CFD_i is the ith annual "Cash-Flow Discount" (CFD) generated by the investment. As shown in the equation Equation (8), the ith CFD can be obtained using the corresponding "Cash-Flow" (CF) and multiplying it to the "Present Value Single Payment". The $PVSP_i$ depends on the "Discount Rate" and provides the discount value of an amount (at the time of the economic analysis) expected at the ith year, by the formula:

$$\mathrm{PVSP}_\mathrm{i} = \frac{1}{(1+\mathrm{r})^\mathrm{i}} \tag{9}$$

Table 11 shows the PVSP (20 year, 2.5%) that was used for the proposed economic assessment.

Table 11. PVSP (20 year, 2.5%).

1	2	3	4	5	6	7	8	9	10
0.9756	0.9518	0.9286	0.9060	0.8839	0.8623	0.8413	0.8207	0.8007	0.7812
11	**12**	**13**	**14**	**15**	**16**	**17**	**18**	**19**	**20**
0.7621	0.7436	0.7254	0.7077	0.6905	0.6736	0.6572	0.6412	0.6255	0.6103

The CF_i is computed considering the annual revenue R_i and the avoided costs AC_i of the ith year due to the investment. In our case of study, the AC_i was computed using the following formula:

$$AC_i = \Delta ST_i + \Delta SB_i \quad (10)$$

where, ΔST_i ("Saving Taxes") are the savings from the taxes (in Italy, the economic discipline allows a deduction from the taxes of 50% of the investment within the first ten years of the PV installation) and ΔSB_i ("Saved Bill") are the savings of the electrical bill:

$$\Delta SB_i = BBI_i - BAB_i \quad (11)$$

where, BBI stands for "Bill Before the Investment" and BAB stands for "Bill after the Investment".

The revenue R_i is a credit provided by the Government to the household owner that depends on the energy exchanged with the grid as ruled by the net-metering regulation [11]. So, the following formula is used:

$$R_i = SSP_i - \Delta VES_i + AFSSP \quad (12)$$

It makes use of the information presented in Tables 8–10 to compute the following variables:

- SSP (credit recognized) = min (OE, CEI) + UFEV × ES;
- OE (value of energy withdrawn from the grid) = E_{FG} × Energy Cost;
- CEI (value of energy injected to the grid) = E_{TG} × Energy Trade Price;
- ES (energy exchanged with the grid) = min (E_{FG}, E_{TG});
- * ΔVES (value of the energy surplus) = CEI − OE, only if CEI > OE (otherwise is 0).

Where AFSSP is the "Annual Fee for SSP" (30 €/y), E_{FG} is the energy withdrawn from the grid and E_{TG} is the energy transferred to the grid.

Tables 12–15 present the results of the cash-flow analysis. It is possible to observe that the NPV (at the 20th year) of a PV system without battery is higher than the same PV system with battery. These results confirm the one shown in [11] that investigated the economic profitability of a PV system during the first 10 years of lifetime.

Table 12. Cash-Flow Analysis—Location 1, PV plant with Battery (cost investment, C_0 = 10,676 €).

Year	AC	R	CFi	CFDi	∑CFDi	Year	AC	R	CFi	CFDi	∑CFDi
1	950	119	1070	1044	1044	11	411	138	549	419	9930
2	958	146	1104	1051	2096	12	391	152	543	404	10,334
3	940	118	1058	983	3079	13	375	164	539	391	10,725
4	965	132	1097	994	4073	14	358	174	532	377	11,102
5	972	137	1109	981	5054	15	342	185	527	364	11,467
6	940	116	1057	912	5966	16	328	196	524	353	11,820
7	943	119	1062	894	6860	17	314	206	521	342	12,163
8	971	134	1105	907	7768	18	303	213	516	331	12,494
9	937	128	1065	853	8621	19	292	220	513	320	12,815
10	979	159	1138	889	9511	20	280	229	510	311	13,127
										NPV	**2451**

Table 13. Cash-Flow Analysis—Location 1, PV plant without Battery (cost investment, C_0 = 7676 €).

Year	AC	R	CFi	CFDi	∑CFDi	Year	AC	R	CFi	CFDi	∑CFDi
1	549	296	846	825	825	11	181	300	481	366	7930
2	559	323	882	840	1666	12	181	300	482	358	8288
3	551	284	836	776	2442	13	183	300	484	351	8640
4	560	314	874	792	3234	14	184	297	481	341	8981
5	563	322	886	783	4018	15	185	297	482	333	9314
6	553	282	836	720	4738	16	186	298	485	326	9641
7	558	283	842	708	5447	17	187	296	484	318	9959
8	568	314	882	724	6171	18	188	295	484	310	10,270
9	550	295	845	677	6849	19	189	293	482	302	10,572
10	574	340	914	714	7563	20	191	293	484	295	10,867
										NPV	**3191**

Table 14. Cash-Flow Analysis—Location 2, PV plant with Battery (cost investment, C_0 = 10,676 €).

Year	AC	R	CFi	CFDi	∑CFDi	Year	AC	R	CFi	CFDi	∑CFDi
1	1007	178	1186	1157	1157	11	470	211	681	519	1,0999
2	1009	175	1185	1128	2285	12	456	227	683	508	11,508
3	992	171	1163	1080	3366	13	440	243	683	496	12,004
4	1003	177	1181	1070	4436	14	419	259	679	480	12,485
5	1015	188	1204	1064	5501	15	399	275	675	466	12,951
6	1011	183	1195	1030	6531	16	384	288	672	453	13,404
7	1016	191	1208	1016	7548	17	367	303	671	441	13,845
8	1010	200	1210	993	8541	18	349	316	666	427	14,272
9	1009	202	1212	970	9512	19	335	325	660	413	14,686
10	1022	216	1238	967	10,480	20	321	334	655	400	15,086
										NPV	**4410 €**

Table 15. Cash-Flow Analysis—Location 2, PV plant without Battery (cost investment, C_0 = 7676 €).

Year	AC	R	CFi	CFDi	∑CFDi	Year	AC	R	CFi	CFDi	∑CFDi
1	575	381	956	933	933	11	202	397	600	457	8927
2	575	381	956	910	1844	12	204	400	604	449	9376
3	566	366	932	866	2710	13	205	403	608	441	9818
4	576	376	952	862	3573	14	206	403	609	431	10,250
5	582	392	974	861	4434	15	207	405	612	423	10,673
6	579	386	965	832	5266	16	209	407	616	415	11,088
7	582	394	977	822	6089	17	210	411	621	408	11,497
8	581	398	980	804	6893	18	211	410	622	399	11,896
9	586	396	982	786	7680	19	213	413	626	392	12,288
10	593	416	1009	788	8469	20	214	410	624	381	12,669
										NPV	**4993**

Making a pair comparison between Tables 12 and 13 for Location 1 and Table 14 vs. Table 15 for Location 2, it is possible to observe that the main economic benefit brought by the installation of a storage solution is the increase of avoided costs. In particular, during the first ten years, the avoided costs depend on the electrical bill reduction and on the tax deduction (Saving Taxes of the 50% of the PV investment). Afterwards, only the electrical bill reduction contributes to the avoided costs. On the other hand, the economic reward (R) of the net-metering service is higher in a PV plant without battery. This result can be expected because, as ruled by Equation (12), in the PV plant equipped with a battery, the amount of energy withdrawn by (and injected to) the electrical grid decreases, and so does the economic value of the net-metering contribution (SSP) and the contribution ΔVES (value of the energy surplus). Unfortunately, the net-metering mechanism, conceived in 2007 to serve PV power plants

without storage systems, does not consider the auto-consumption as an added value and does not reward the usage of the stored energy.

Figure 18 shows the "return of investment" trend. This figure allows the identification of the pay-back time for the four investments proposed in Table 7, considering respectively the PV system with and without battery in both the locations. In particular, it is possible to notice that the PV system without battery in Location 2 returned during the 9th year of activity, whereas the same configuration for Location 1 took two more years. The PV systems with battery required respectively 13 and 11 years to return in Location 1 and Location 2.

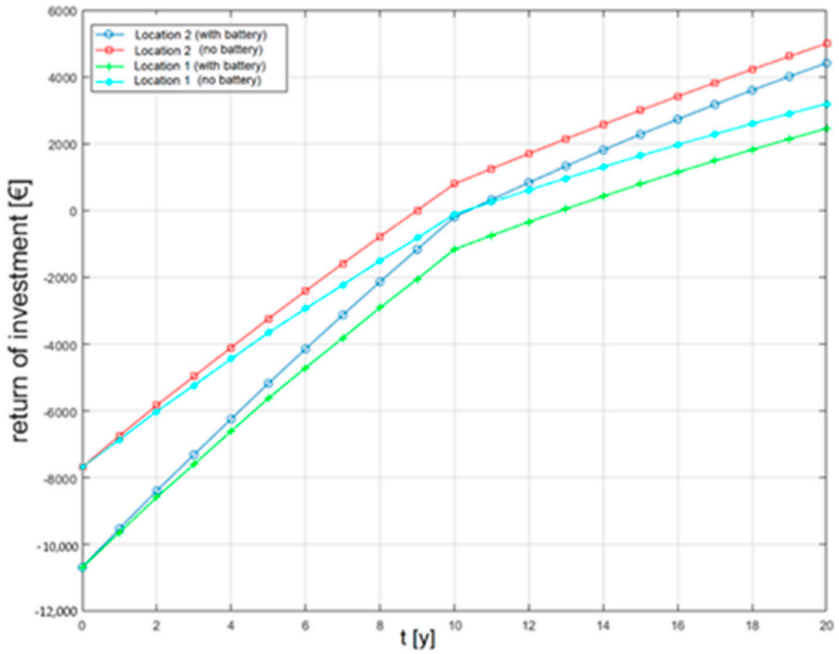

Figure 18. The return of investment.

The results so far shown have demonstrated that, in Italy the current market scenario is not yet favorable for the installation of a battery in domestic PV applications. In order to understand what conditions can turn the market in favor of the installation of the battery, a sensitivity analysis was performed. Figures 19 and 20 show how the payback time and the NPV change with a variation of the battery cost per kWh (from 500 to 100 €/kWh).

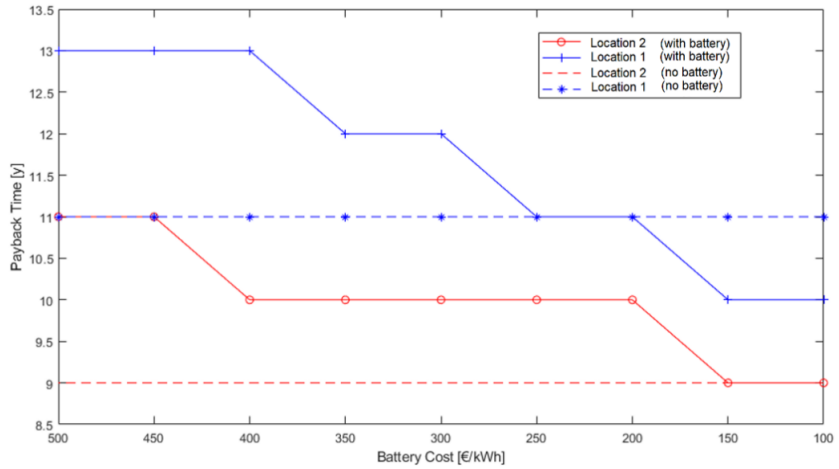

Figure 19. Payback time sensitivity analysis with respect to a variation of the battery cost.

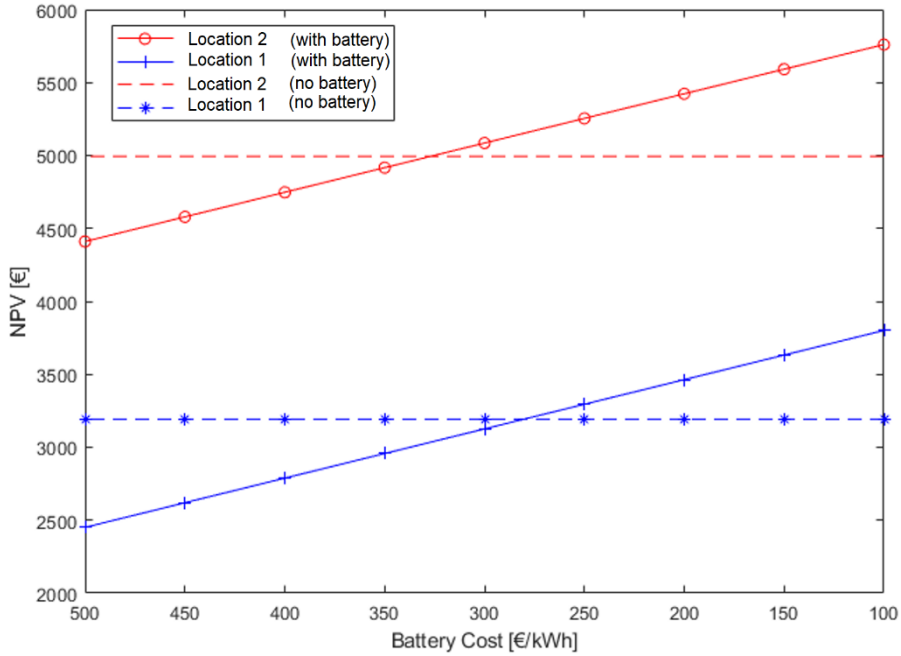

Figure 20. Net Present Value (NPV) (20th year) sensitivity analysis with respect to a variation of the battery cost.

As far as it concerns the payback time, Figure 19 shows that the cost of the battery must decrease to 200 €/kWh and 150 €/kWh, respectively, for the Location 1 and Location 2, in order to equalize the investment of a PV system without battery. Instead, Figure 20 reveals that the installation of a storage system starts to become more profitable (than the same PV plant without battery) for where the costs of the battery is lower than 300 €/kWh. In this case, the payback time would occur, respectively in Location 1 and Location 2, at the 12th and at the 10th year from the beginning of the investment.

5. Conclusions

In this paper, a performance and an economic evaluation of storage systems in domestic grid-connected PV power plants was presented. The analysis was carried out considering two different locations, in the north and in the south of Italy, characterized by different environmental conditions. The model developed with the SHyFTA technique was allowed to consider the main physical mathematical equations of the photovoltaic energy conversion and the stochastic behavior of the PV system. In this way, it was possible to simulate the PV systems using the real historical series of the ambient temperature and of the irradiation (for both locations) of the last ten years. Moreover, thanks to the SHyFTA model, the failures, the aging and maintenance of the system components (including the PV panels, the inverter and the storage system) were also taken into account, in order to obtain a more realistic simulation than traditional deterministic models.

The results of the performance evaluation revealed that a PV power plant of 3 kW_p—assuming the best installation condition (for both locations)—in the south of Italy can be enough to satisfy an energy demand of 4300 kWh/year, whereas it cannot cover—in the north of Italy—a domestic consumption higher than 3500 kWh/year. Moreover, the simulations showed that the installation of a storage system of 6.5 kWh of capacity can increase the auto-consumption up to the 60–65%, no matter the location. This demonstrates that the grid-connected architecture is still the most appropriate design solution for domestic applications, because they can guarantee the energy supply with a service availability of 98.5%, avoiding undesired service shortage that can occur in a stand-alone configuration.

Although the installation of the energy storage systems may seem a promising investment for private consumers, the results of the economic evaluation reveal very interesting information. Assuming the main characteristics of the Italian market, the economic evaluation was carried out for

twenty years (extending the time-series of ten years) which is the typical useful-life of a PV power plant. Based on the current Italian regulations for the grid-connected PV plant within the net-metering regime, an economic comparison between an investment of a traditional PV plant without and with battery was performed. The results demonstrated that the economic advantages of Li-ion storage systems of grid-connected PV applications were not yet remarkable if compared with the investment of a traditional PV power plant. In fact, the NPV (at the twentieth year) of a PV system without storage system was higher than the equivalent PV system with battery. A sensitivity analysis for evaluating what market conditions can favor the installation of a storage systems showed that a cost decrease of the 70% is required (from the current 500 to 200 ÷ 150 €/kWh) to make the installation of the storage systems economically convenient.

In the authors' opinion, the reasons of this economic debacle are linked with the lack of a specific regulation for grid-connected PV power plants equipped with a storage system. Such systems, at the state of the art, must adhere to the old net-metering regulations for grid-connected PV plants (without storage system), conceived in the early 2007 (and updated in 2016 [33]). The latter, in fact, does not reward the auto-consumption and, in addition, decreases the quota of the SSP credit linked to the energy exchanged with the grid that is drastically reduced in the architecture including a storage system. In conclusion, storage technology represents an advancement in the PV applications, but its breakthrough must be accompanied by an important cost decrease and must be favored by dedicated mechanisms of incentives and management regulations.

Author Contributions: F.C. conceived the methodology and performed the economic assessment; F.F. conceived the methodology and implemented the case of study; D.D. verified the correctness of the methodology and of the economic assessment; L.C. reviewed the methodology, validated the model and verified the coherence of the simulation results.

Funding: This research received no external funding.

Conflicts of Interest: The authors declare no conflict of interest.

Nomenclature

AC	Avoided Costs	(€/y)
AFSSP	Annual Fees of Net-Metering Service	(€/y)
BAB	Bill After Investment	(€/y)
BBI	Bill Before Investment	(€/y)
CF	Cash Flow	(€/y)
CFD	Cash Flow Discount	(€/y)
DoD	Depth of Discharge	(%)
DPBT	Discounted Payback Time	
E_B	Energy from the battery	(kWh)
E_{DD}	Daily Energy demand	(kWh)
E_{FG}	Energy from the GRID	(kWh)
E_L	Energy Loss	(kWh)
E_{PV}	Energy from PV plant	(kWh)
E_S	Battery Energy stored	(kWh)
ES	Energy Exchanged with the Grid	(kWh)
E_{TG}	Energy to the GRID	(kWh)
FIT	Feed-in Tariff	
G	Global Irradiance	(W/m^2)
HV	High Voltage	
I	Irradiance	(kWh)
LV	Low Voltage	
LCOE	Levelized Cost of Electricity	
IG_y	Yearly Global Irradiance	(kWh/m^2)
NPV	Net Present Value	(€)
PV	Photovoltaic	

P_L	Load Power demand	(W)
PM_{peak}	Module power peak	(kW)
P_{peak}	Overall power peak system	(kW)
R	Revenue due to the investment	(€/y)
SB	Saved Bill	(€/y)
SoC	State of Charge	(%)
SSP	Net-Metering subsidy	(€/y)
ST	Saving Taxes	(€/y)
T_a	Ambient air Temperature	(°C)
T_C	Module Temperature	(°C)
VES	Value of the Energy Surplus	(€/y)

References

1. Alstone, P.; Gershenson, D.; Kammen, D.M. Decentralized energy systems for clean electricity access. *Nat. Clim. Chang.* **2015**, *5*, 305. [CrossRef]
2. Regola Tecnica di Riferimento per la Connessione di Utenti Attivi e Passivi alle Reti AT ed MT Delle Imprese Distributrici di Energia Elettrica. Available online: https://nt24.it/app/uploads/2017/09/Norma-CEI-0-16-2014.pdf (accessed on 16 May 2019).
3. Cucchiella, F.; D'Adamo, I. Feasibility study of developing photovoltaic power projects in Italy: An integrated approach. *Renew. Sustain. Energy Rev.* **2012**, *16*, 1562–1576. [CrossRef]
4. Edalati, S.; Ameri, M.; Iranmanesh, M.; Tarmahi, H.; Gholampour, M. Technical and economic assessments of grid-connected photovoltaic power plants: Iran case study. *Energy* **2016**, *114*, 923–934. [CrossRef]
5. Bakhshi, R.; Sadeh, J. Economic evaluation of grid–connected photovoltaic systems viability under a new dynamic feed–in tariff scheme: A case study in Iran. *Renew. Energy* **2018**, *119*, 354–364. [CrossRef]
6. Cucchiella, F.; D'Adamo, I.; Gastaldi, M. Economic analysis of a photovoltaic system: A resource for residential households. *Energies* **2017**, *10*, 814. [CrossRef]
7. Akinyele, D.O.; Rayudu, R.K.; Nair, N.K.C. Development of photovoltaic power plant for remote residential applications: The socio-technical and economic perspectives. *Appl. Energy* **2015**, *155*, 131–149. [CrossRef]
8. Mohammadi, K.; Naderi, M.; Saghafifar, M. Economic feasibility of developing grid-connected photovoltaic plants in the southern coast of Iran. *Energy* **2018**, *156*, 17–31. [CrossRef]
9. Kairies, K.P.; Figgener, J.; Haberschusz, D.; Wessels, O.; Tepe, B.; Sauer, D.U. Market and technology development of PV home storage systems in Germany. *J. Energy Storage* **2019**, *23*, 416–424. [CrossRef]
10. Akinyele, D.; Belikov, J.; Levron, Y. Battery storage technologies for electrical applications: Impact in stand-alone photovoltaic systems. *Energies* **2017**, *10*, 1760. [CrossRef]
11. Abdin, G.C.; Noussan, M. Electricity storage compared to net metering in residential PV applications. *J. Clean. Prod.* **2018**, *176*, 175–186. [CrossRef]
12. Firouzjah, K.G. Assessment of small-scale solar PV systems in Iran: Regions priority, potentials and financial feasibility. *Renew. Sustain. Energy Rev.* **2018**, *94*, 267–274. [CrossRef]
13. Chiacchio, F.; D'Urso, D.; Aizpurua, J.I.; Compagno, L. Performance assessment of domestic photovoltaic power plant with a storage system. *IFAC-PapersOnLine* **2018**, *51*, 746–751. [CrossRef]
14. Manno, G.; Zymaris, A.; Kakalis, N.P.; Chiacchio, F.; Cipollone, G.; Compagno, L.; D'Urso, D.; Trapani, N. Dynamic reliability of three nonlinear aging components with different failure modes characteristics. In Proceedings of the European Safety and Reliability Conference (ESREL), Amsterdam, The Netherlands, 29 September 2013; pp. 3047–3055.
15. Devooght, J. Dynamic reliability. *Adv. Nucl. Sci. Technol.* **2002**, *25*, 215–278.
16. Truong, C.; Naumann, M.; Karl, R.; Müller, M.; Jossen, A.; Hesse, H. Economics of residential photovoltaic battery systems in Germany: The case of Tesla's Powerwall. *Batteries* **2016**, *2*, 14. [CrossRef]
17. Chiacchio, F.; D'Urso, D.; Compagno, L.; Pennisi, M.; Pappalardo, F.; Manno, G. SHyFTA, a stochastic hybrid fault tree automaton for the modelling and simulation of dynamic reliability problems. *Expert Syst. Appl.* **2016**, *47*, 42–57. [CrossRef]
18. Chiacchio, F.; D'Urso, D.; Famoso, F.; Brusca, S.; Aizpurua, J.I.; Catterson, V.M. On the use of dynamic reliability for an accurate modelling of renewable power plants. *Energy* **2018**, *151*, 605–621. [CrossRef]

19. Chiacchio, F.; Famoso, F.; D'Urso, D.; Brusca, S.; Aizpurua, J.I.; Cedola, L. Dynamic performance evaluation of photovoltaic power plant by stochastic hybrid fault tree automaton model. *Energies* **2018**, *11*, 306. [CrossRef]
20. Urtasun, A.; Sanchis, P.; Marroyo, L. Limiting the power generated by a photovoltaic system. In Proceedings of the 2013 10th International Multi-Conference on Systems, Signals and Devices, Hammamet, Tunisia, 18–21 March 2013. [CrossRef]
21. Skoplaky, E.; Palyvos, J.A. Operating temperature of photovoltaic modules: A survey of pertinent correlations. *Renew. Energy* **2009**, *34*, 23–29. [CrossRef]
22. Smith, K.; Saxon, A.; Keyser, M.; Lundstrom, B.; Cao, Z.; Roc, A. Life prediction model for grid-connected li-ion battery energy storage system. In Proceedings of the American Control Conference, Seattle, WA, USA, 24–26 May 2017.
23. Christensen, J.; Newman, J. A mathematical model of stress generation and fracture in lithium manganese oxide. *J. Electrochem. Soc.* **2006**, *153*, A1019–A1030. [CrossRef]
24. Deshpande, R.; Verbrugge, M.; Cheng, Y.T.; Wang, J.; Liu, P. Battery cycle life prediction with coupled chemical degradation fatigue mechanics. *J. Electrochem. Soc.* **2012**, *159*, A1730–A1738. [CrossRef]
25. Wang, J.; Liu, P.; Hicks-Garner, J.; Sherman, E.; Soukiazian, S.; Verbrugge, M.; Tataria, H.; Musser, J.; Finamore, P. Cycle-life model for graphite-LiFePO4 cells. *J. Power Sources* **2011**, *196*, 3942–3948. [CrossRef]
26. Peterson, S.B.; Apt, J.; Whitacre, J.F. Lithium-ion battery cell degradation resulting from realistic vehicle and vehicle-to-grid utilization. *J. Power Sources* **2010**, *195*, 2385–2392. [CrossRef]
27. Schmalstieg, J.; Kabitz, S.; Ecker, M.; Sauer, D.U. A holistic aging model for Li(NiMnCo)O2 based 18650 lithium-ion batteries. *J. Power Sources* **2014**, *257*, 325–334. [CrossRef]
28. Santhanagopalan, S.; Smith, K.; Neubauer, J.; Kim, G.H.; Pesaran, A.; Keyser, M. *Design and Analysis of Large Lithium-Ion Battery Systems*; Artech House: Boston, MA, USA, 2015.
29. Stroe, D.I.; Swierczynski, M.; Stroe, A.I.; Teodorescu, R.; Laerke, R.; Kjaer, P.C. Degradation behaviour of Lithium-ion batteries based on field measured frequency regulation mission profile. In Proceedings of the IEEE Energy Conversion Congress and Exposition, Montreal, QC, Canada, 20–24 September 2015.
30. Servizio Informativo Agrometeorologico Siciliano. Available online: http://www.sias.regione.sicilia.it/ (accessed on 16 May 2019).
31. ARPA Lombardia. Available online: http://www.arpalombardia.it/Pages/ARPA_Home_Page.aspx (accessed on 16 May 2019).
32. Aizpurua, J.I.; Catterson, V.M.; Papadopoulos, Y.; Chiacchio, F.; D'Urso, D. Supporting group maintenance through prognostics-enhanced dynamic dependability prediction. *Reliab. Eng. Syst. Saf.* **2017**, *168*, 171–188. [CrossRef]
33. GSE Regole Tecniche Per L'attuazione Delle Disposizioni Relative All'integrazione Di Sistemi Di Accumulo Di Energia Elettrica Nel Sistema Elettrico Nazionale (ai sensi della deliberazione 574/2014/R/eel e s.m.i). 2016. Available online: https://www.gse.it/documenti_site/Documenti%20GSE/Servizi%20per%20te/SISTEMI%20DI%20ACCUMULO/Normativa/Regole%20Tecniche.PDF (accessed on 16 May 2019).